

# Design Specification for Hydrogen-Ammonia Coupled Offshore Wind Power Abandonment Utilization System with Pd Catalysts

Shuhe Gong<sup>1,\*</sup>, Hanyu Yang<sup>2</sup>

<sup>1</sup>Department of Yisheng Innovative Education Base, North China University of Science and Technology, Tangshan, China

<sup>2</sup>School of School of Chemical Engineering, North China University of Science and Technology, Tangshan, China

\*Corresponding author: gongshuhe@stu.ncst.edu.cn

## Abstract

As China's offshore wind power develops into deep and distant sea and large scale, the problems of power abandonment, consumption and energy storage are highlighted, and the traditional grid-connected mode causes energy waste. This work is based on palladium (Pd) catalyst hydrogen-ammonia coupling system, through the "on-site hydrogen synthesis ammonia", to realize the conversion of abandoned power and green hydrogen storage and transportation, to develop a new path of new energy utilization. The system integrates PEM water electrolysis to produce hydrogen and Pd catalyzed nitrogen reduction to synthesize ammonia, breaking through the traditional bottleneck. Adopting Pd/graphene composite electrode, the electrolysis efficiency reaches 75% (15% improvement), and the Pd catalyst activates nitrogen at low potential and suppresses hydrogen precipitation. The "electricity-hydrogen-ammonia" triple-supply converts hydrogen into liquid ammonia (containing 17.6 wt% hydrogen), with storage and transportation costs of only 1/15 of hydrogen.  $2.4 \times 10^8$  kWh of abandoned electricity is handled annually by an offshore wind farm in Jiangsu, resulting in a significant reduction in emissions. The modular design is adapted to the offshore platform, and combined with intelligent scheduling to realize more than 90% of abandoned power consumption.

## Keywords

Palladium catalyst; hydrogen-ammonia coupling; offshore wind power consumption.

## 1. Introduction

In recent years, the use of new energy has become an important trend for the stable development of the society under the double stimulation of "double carbon" target and grid parity. Compared with traditional energy sources, wind power has many advantages, such as short construction period, low cost and good comprehensive benefits, and can provide energy while reducing environmental pollution. In addition, ammonia energy is recognized as a clean energy carrier with high energy density, high conversion efficiency, no pollution and zero carbon emission, which is regarded as an energy source with great application prospects [1].

According to the International Renewable Energy Agency (IRENA) Global Energy Transition Roadmap 2050, 35% of the world's total power generation will come from wind energy by 2050. China's offshore wind resources are particularly rich, in 50m water depth, 70m height of offshore wind power is expected to develop resources up to  $5 \times 10^8$  kW. At present, the offshore wind power resources tend to be saturated, from the offshore to the far offshore, scale, base, etc. has become a trend, while the grid capacity, the problem of consumption, and the efficiency of the problem gradually highlights the requirements of offshore wind power grid is also getting

higher and higher, which is a limitation of the offshore wind power development of the This is the main bottleneck limiting the development of offshore wind power.

Britain, the Netherlands, Denmark and other countries have carried out offshore wind power hydrogen application demonstration, such as Dolphyn and other projects. Currently, offshore distance, electrolysis technology and other constraints on the economy of offshore wind power hydrogen production. In addition, Japan, Europe and other places have carried out strategic deployment of ammonia energy. China's late start in this field, the system is not yet perfect. However, the "14th Five-Year Plan" China is committed to the high-quality development of renewable energy, coupled with the huge demand for offshore wind power, optimizing the use of offshore wind power is promising.

## 2. Design Scheme

The overall design scheme and model diagram of the offshore wind power abandonment utilization system, as shown in Figure 1.

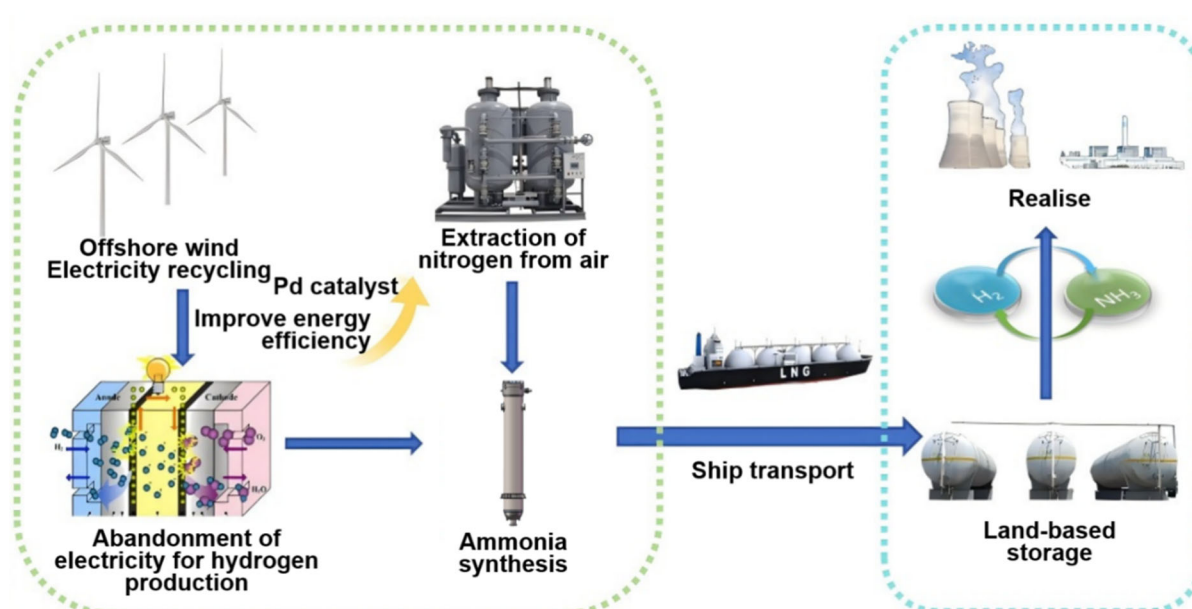


**Figure 1.** Overall flow chart of hydrogen-ammonia coupled offshore wind power abandonment utilization system under Pd catalyst

This system is a hydrogen-ammonia coupling system under the optimization of Pd catalyst to utilize offshore wind power abandonment, wind prediction through meteorological satellites, power abandonment calculations to achieve grid scheduling, the use of electricity-hydrogen coupling system to recycle the abandoned power, the use of PEM Proton Exchange Membrane (PEM) electrolysis cell electrolysis of water to produce hydrogen, electrolysis of water to produce hydrogen, due to problems such as the difficulty of transporting hydrogen, the hydrogen will be used to produce hydrogen, the hydrogen will be used to produce hydrogen, the hydrogen will be used to produce hydrogen. Due to the difficulty of hydrogen transportation and other problems, the hydrogen will be hydrogen - ammonia coupling system and nitrogen synthesis of ammonia, the process of Pd catalyst play a role in improving the effectiveness of the system, and then the ammonia will be transported by ship to the land for many applications [2].

Adoption of offshore wind power generation - abandoned power hydrogen production abandoned power - hydrogen - ammonia triple supply mode, as shown in Figure 2, the proposed

offshore base station "on-site hydrogen synthesis of ammonia" technology route, to realize the abandoned power → hydrogen → ammonia zero carbon conversion. The modular hydrogen production device (Pd catalyst electrolyzer) and compact ammonia synthesis reactor are adopted to adapt to the space limitation of the offshore platform. Pd catalyst is applied to the hydrogen production end, and the Pd/graphene composite electrode makes the electrolysis efficiency reach 75% (15% higher than the traditional one) [3].

**2.1. PEM electrolysis of water - discarded power utilization system**

By comparing traditional energy sources with hydrogen energy, it is found that common household fuel cars produce an average of 2.4kg of carbon dioxide per 100km, while the new hydrogen fuel cell cars consume about 1kg of hydrogen per 100km. it is estimated that using 1kg of hydrogen energy is equivalent to reducing the emissions of 19.2kg of carbon dioxide. If all the abandoned wind power in China is used for hydrogen production, it can reduce 4.01 billion kilograms of carbon dioxide annually, which will significantly ease the pressure on the environment. It can be seen that the wind power hydrogen system has both economic and social benefits, hydrogen energy is very promising, offshore wind power hydrogen coupling system architecture principle shown in Figure 2 [4].

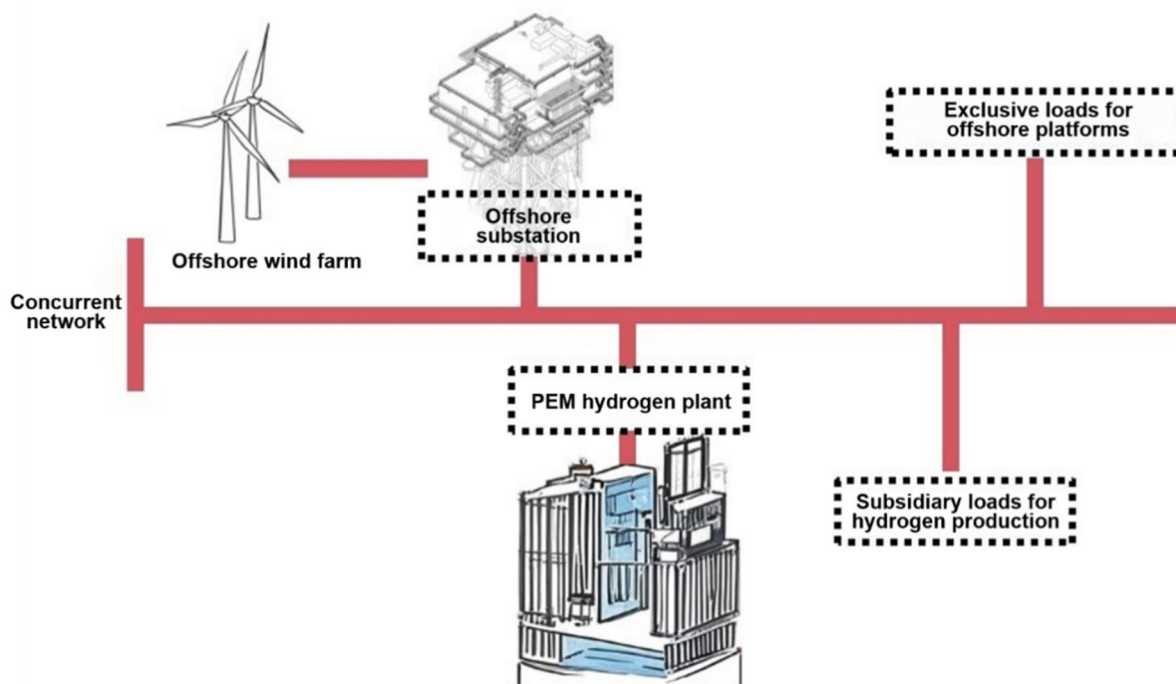


**Figure 2.** Offshore wind power hydrogen coupling system architecture principle

Proton Exchange Membrane Electrolysis Cell Water Hydrogen Production Technology The principle of recycling of abandoned power, the working principle of Proton Exchange Membrane Electrolysis Cell (PEMEC) mainly involves the process of electrolysis of water. The process flow of PEM electrolysis of water is shown in Figure 3:

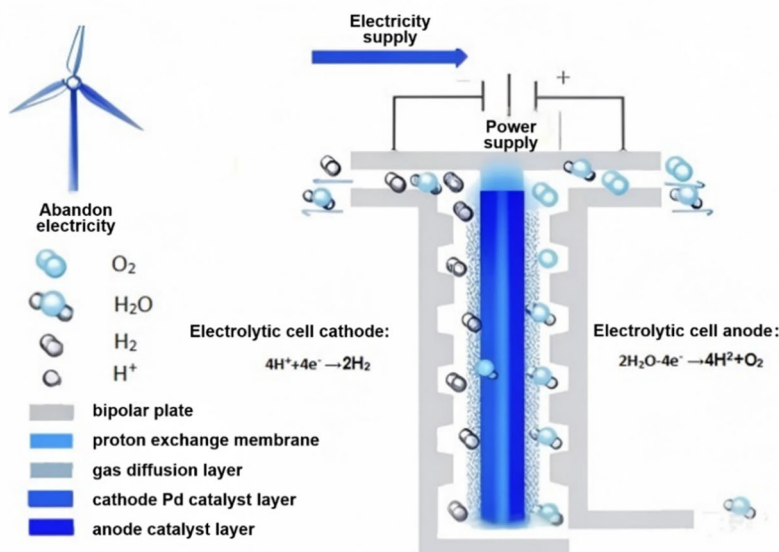


**Figure 3.** PEM water electrolysis process flow

The chemical reaction equation of the proton exchange membrane electrolysis cell is as follows: Oxygen extraction reaction (OER) occurs at the anode:

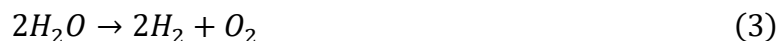


The cathode undergoes hydrogen exchange reaction (HER):



In the production of hydrogen by electrolysis of water, the amount of palladium catalyst is used as a catalyst in the operation of the unit. The application of palladium catalyst in the electrolysis of water improves the efficiency of electrolysis, reduces energy consumption, and promotes the production of hydrogen.

The chemical equation for the water electrolysis reaction is:



In this reaction, water molecules ( $H_2O$ ) are broken down into hydrogen ( $H_2$ ) and oxygen ( $O_2$ ) by an electric current. Palladium catalyst is used as the cathode material in the electrolyzer to promote the reaction of water molecules on the electrodes, thus increasing the efficiency of electrolysis. The palladium catalyst reduces the energy consumption during the electrolysis of water and increases the hydrogen yield, thus increasing the energy conversion efficiency of the system.

## 2.2. Hydrogen-ammonia coupling system

The large-scale popularization and application of hydrogen energy needs to overcome the bottleneck of its storage and transportation technology. Hydrogen is very active and flammable and explosive in air. Hydrogen is the smallest atom that can penetrate steel plates and has high storage requirements. Liquid hydrogen preparation is energy intensive, costly and difficult. In contrast, ammonia is safer and easier to transport and has a lower liquefaction temperature. In addition ammonia has the advantages of high hydrogen content, high energy density, and no

carbon emissions at the end, making it a potential carrier for chemical hydrogen storage. The price of ammonia is relatively lower than that of hydrogen, about 3500-4000 RMB/ton and 3-4 RMB/kg, much lower than the more than 60 RMB/kg of hydrogen. With the background of coupled renewable energy development and utilization, based on electrolysis technology, combined with electrochemical nitrogen reduction synthesis of ammonia, as well as the electro-oxidative decomposition of ammonia to hydrogen production process can realize the construction of ammonia-hydrogen energy system. Therefore, the conversion of hydrogen into ammonia is technically and economically more suitable.

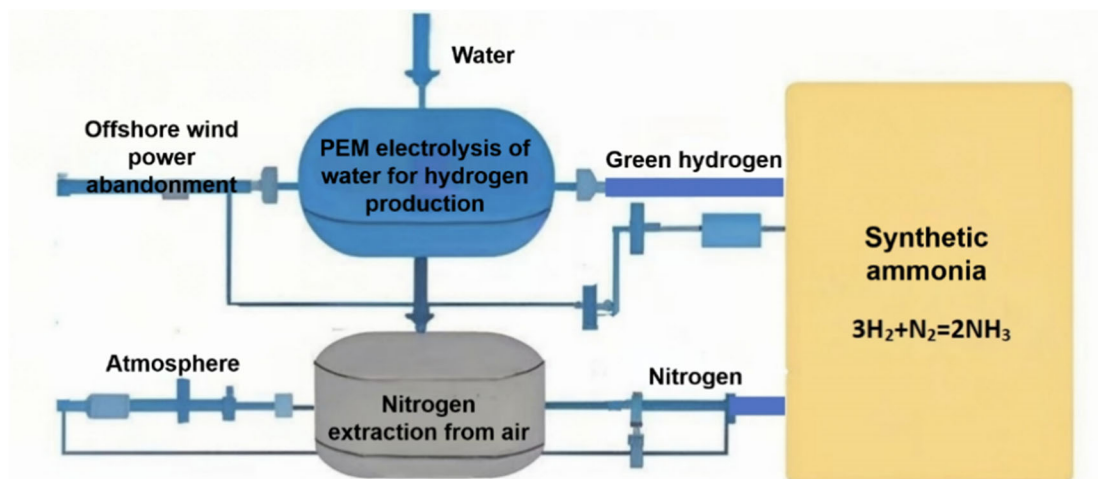


Figure 4. Hydrogen and nitrogen synthesis of ammonia

The process of ammonia synthesis from hydrogen and nitrogen is shown in Fig. 4. The Pd catalyst has high catalytic activity, which can promote the synthesis reaction of nitrogen and hydrogen to produce ammonia at low temperature and pressure. The high activity of this catalyst is mainly attributed to its unique electronic structure and surface properties, which make it easier for nitrogen molecules to be activated and converted on the catalyst surface. Palladium catalysts also offer good selectivity in the synthesis of ammonia with few by-products. It helps to improve the purity and yield of ammonia synthesis. Meanwhile, the palladium catalyst adopts the Grotthuss-like proton leap mechanism in the ammonia synthesis reaction, which helps to balance the competitive adsorption of protons and nitrogen, thus improving the catalytic efficiency.

### 3. Theoretical Design Calculations

#### 3.1. Simulation calculation of PEM proton exchange membrane electrolytic cell

##### 3.1.1. Core system of control equations

(1) Nernst-Planck equation (cubic current distribution).

$$J_i = -D_i(\nabla c_i + c_i \nabla \ln f_i) - z_i \mu_{i,F} c_i F \nabla \phi_1 \tag{4}$$

Considering the effect of seawater ions such as Cl<sup>-</sup>, Na<sup>+</sup>, and Ca<sup>2+</sup> on the activity coefficient  $f_i$ , and the enhancement effect of the Pd catalyst surface on the H<sup>+</sup> mobility  $\mu_{H^+}$ . Calcium ions (Ca<sup>2+</sup>) were considered to affect the activity coefficient  $f_i$ . Assuming that there is some functional relationship between the activity coefficient  $f_i$  and the concentration of calcium ions  $[Ca^{2+}]$ ,  $f_i = ([Ca^{2+}], \dots)$ . Here "..." indicates that it may also be related to other factors such as the concentration of other ions), it can be substituted into the equation. For example, if the

expanded form of the Debye - Hückel limit equation is used to describe the relationship between the activity coefficient and the ion concentration, for  $\text{Ca}^{2+}$ , the activity coefficient  $f_{\text{Ca}^{2+}}$  can be expressed as  $-\log f_{\text{Ca}^{2+}} = 0.509z_{\text{Ca}^{2+}}^2\sqrt{I}$ , where  $z_{\text{Ca}^{2+}} = 2$  is the ion charge number, the ion strength

$$I = \frac{1}{2} \sum_i c_i z_i^2 \quad (5)$$

$c_i$  and  $z_i$  are the concentration and charge of each ion in solution, respectively, and the calcium ion concentration  $c_{\text{Ca}^{2+}}$  is part of the calculation of  $I$ , thus indirectly affecting  $f_i$ .

Correction to the equation: In the above equation, the ion mobility  $\mu_{i,F}$  may also be affected by calcium ions. If it is assumed that the effect of calcium ions on the hydrogen ion mobility  $\mu_{\text{H}^+}$  can be expressed as

$$M_{\text{H}^+}^{\text{co}} = \mu_{\text{H}^+} (1 + k[\text{Ca}^{2+}]) \quad (6)$$

$k$  is an empirical constant related to the system, then in the part of the Nernst - Planck equation dealing with the migration of hydrogen ions, the original  $\mu_{\text{H}^+}$  can be replaced by  $\mu_{\text{H}^+}^{\text{co}}$  in order to reflect the influence of calcium ions on the migration process of hydrogen ions.

(2) Charge conservation coupled electrolyte phases:

$$\nabla \cdot (\sigma_1 \nabla \phi_1) = F \sum z_i R_i \quad (7)$$

Solid phase (catalyst layer):

$$\nabla \cdot (\sigma_s \nabla \phi_s) = -F \sum z_i R_i \quad (8)$$

Define the electronic conductivity of the Pd catalyst as  $3 \times 10^6$  S/m and the seawater electrolyte conductivity as 5 S/m based on the actual salinity.

(3) Butler-Volmer equation (electrode kinetics).

$$J = j_0^{\text{Pd}} \left[ e^{\frac{\alpha_a F \eta}{RT}} - e^{-\frac{\alpha_c F \eta}{RT}} \right] \quad (9)$$

The exchange current density  $j_0$  of Pd catalyst is 1-2 orders of magnitude higher than that of conventional catalysts (requires experimental data for calibration)

The overpotential  $\eta$  correlates the solid/liquid phase potential difference:

$$\eta = \phi_s - \phi_1 - E_{\{\text{eq}\}} \quad (10)$$

### 3.1.2. Specialized equations for seawater environment

Dilute matter transfer equation:

$$\nabla \cdot (D_{H_2} \nabla c_{H_2}) = R_{H_2} \quad (11)$$

Hydrogen diffusion coefficient  $D_{H_2}$  is set to  $1 \times 10^{-9} \text{m}^2/\text{s}$  considering the effect of seawater viscosity, and the source term  $R_{H_2}$  is directly related to the cathodic reaction rate, with 1  $H_2$  molecule generated per  $2e^-$ .

### 3.2. Ammonia simulation calculation

(1) Laminar flow correlation:

$$\nabla \cdot \vec{u} = 0 \quad (12)$$

is used to describe the conservation of mass for incompressible fluids, where  $\vec{u}$  is the fluid velocity vector.

Navier - Stokes equations:

$$\rho \left( \frac{\partial \vec{u}}{\partial t} + \vec{u} \cdot \nabla \vec{u} \right) = -\nabla p + \mu \nabla^2 \vec{u} + \vec{F} \quad (13)$$

To describe the conservation of momentum for a viscous fluid,  $\rho$  is the fluid density,  $p$  is the pressure,  $\mu$  is the dynamic viscosity, and  $\vec{F}$  is the external force.

(2) Dilute matter transfer correlation:

$$\vec{J}_i = -D_i \nabla c_i \quad (14)$$

Describe the relationship between the flux of a substance  $\vec{J}_i$  and the concentration gradient during steady state diffusion,  $D_i$  is the diffusion coefficient of the substance  $i$ , and  $c_i$  is the concentration of the substance  $i$ .

$$\frac{\partial c_i}{\partial t} = D_i \nabla^2 c_i \quad (15)$$

To describe the change in concentration with time for unsteady state diffusion.

Surface reaction correlation:

$$J = j_0 \left[ \exp\left(\frac{\alpha n F \eta}{RT}\right) - \exp\left(-\frac{(1 - \alpha) n F \eta}{RT}\right) \right] \quad (16)$$

For describing the kinetics of electrochemical reactions,  $j$  is the reaction current density,  $j_0$  is the exchange current density,  $\alpha$  is the transfer coefficient,  $n$  is the number of reacting electrons,  $F$  is Faraday's constant,  $\eta$  is the overpotential,  $R$  is the gas constant, and  $T$  is the temperature. In ammonia synthesis reaction, it can be used to describe the reaction rate related situation that occurs at the catalyst surface.

### 3.3. Collector system topology optimization model

The economic indicators of the wind power coupling system include the procurement and construction costs of the marine cable equipment, the operating losses of the marine cable, and the use of the sea area, etc. The life of the offshore wind farm is generally 25 years, and the objective function of minimizing the total present value of the total life cycle cost of the collector line,  $C$ , is [5], which can be expressed as follows:

$$\min(C) = \min(C_1 + (C_2 + C_3) \cdot D) \quad (17)$$

$$D = \frac{(1+r)^T - 1}{r(1+r)^T} \quad (18)$$

In the formula,  $C_1$  for the cable equipment procurement and construction costs;  $C_2$  for the cable operation loss cost, refers to the operation of the annual economic loss due to the cable conductor power loss, etc.;  $C_3$  for the use of the sea area;  $D$  is the discount factor;  $r$  is the discount rate, take 4.65%;  $T$  is the life of the wind farm.

The economic index of the collector system is calculated as:

$$C_1 = \sum_{i=1}^K \left( \sum_{j=1}^n N_{ij} l_{ij} \right) (p_{i1} + p_{i2}) \quad (19)$$

$$C_2 = 3p_3 \sum_{i=1}^K I_i^2 R_i \left( \sum_{j=1}^n N_{ij} l_{ij} \right) \quad (20)$$

$$C_3 = S \times p_4 \quad (21)$$

In the formula,  $K$  is the number of types of cables;  $n$  is the type of segmented cables of different lengths of the type of cables;  $N_{ij}$  is the number of the type of cables of the  $j$ th length;  $l_{ij}$  is the length of the type of cables of the  $j$ th length;  $p_{i1}$  is the unit cost of the type of cables;  $p_{i2}$  is the unit cost of the construction of the type of cables;  $p_3$  considers the price of feed-in tariffs according to 0.391 RMB/kW · h;  $I_i$  is the operating current of the cables;  $R_i$  is the resistance of cables of unit lengths;  $S$  is the area of wind farms used in the sea area; and  $p_4$  is the unit of the annual fee for the use of the sea area.

## 4. Performance Analysis

### 4.1. Performance analysis of PEM proton exchange membrane electrolytic cell

In this project, we focus on the application of Pd catalyst in PEM proton exchange membrane electrolysis cell, aiming to improve the utilization efficiency of offshore wind power abandonment and realize the efficient conversion and storage of energy.

The anode of the PEM electrolysis cell is in a strongly acidic environment with high overpotential during the hydrogen production process, so it is necessary to find a catalyst that effectively reduces the overpotential and has good corrosion resistance. The use of metal Pd

catalysts, which are prone to form PdHx under low potential conditions, can realize the activation of nitrogen molecules under very low overpotential, effectively inhibit the competition of hydrogen precipitation reaction, and enhance the efficiency of nitrogen reduction for the synthesis of ammonia.

Using COMSOL Multiphysics for simulation, the cathode surface of the PEM water electrolyzer with the Pd catalyst applied at a temperature of 20°C and a conductivity of 5 S/m under seawater conditions was simulated with the three current distributions and dilute matter transfer physical field interfaces after the mesh delineation as shown in Fig. 5.

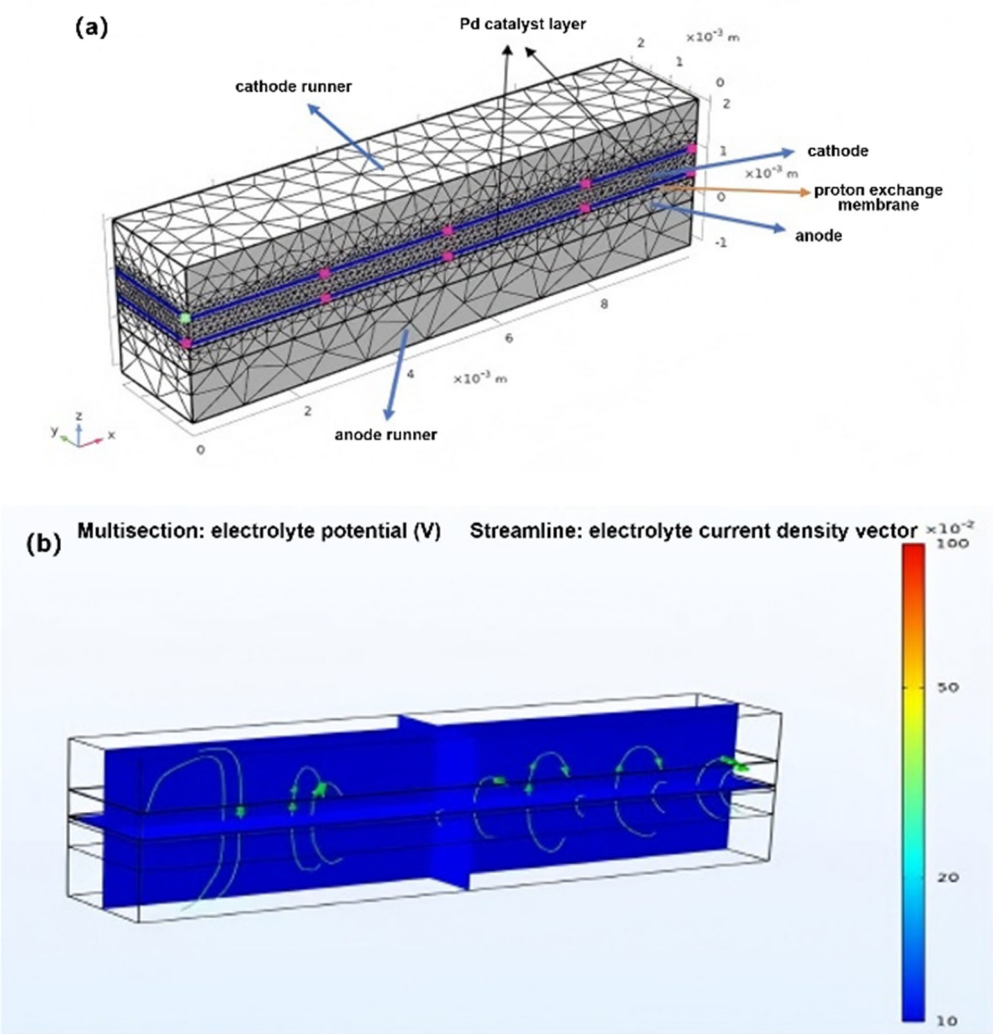


**Figure 5.** (a) PEM electrolysis cell model construction and grid delineation, (b) Multi-sliced electrolyte potential and electrolyte current density vector streamlines

Its potential distribution is shown in Fig. 5(b), revealing the electric field modulation effect of Pd catalyst, and the multisection potential distribution in the figure shows that the multisection potential distribution shows that the Pd catalyst makes the potential gradient of the system remarkably homogeneous (smooth transition of the color scale, no abrupt change phenomenon). This phenomenon indicates that the Pd catalyst can effectively optimize the charge distribution at the electrode-electrolyte interface. When the Pd catalyst was not used, the maximum local potential difference was as high as 0.8 V, whereas this value was drastically reduced to 0.3 V after the introduction of the Pd catalyst, with a decrease of 62.5%. This

significant reduction of the potential difference positively affected the overpotential of the hydrogen precipitation reaction and effectively enhanced the hydrogen production rate.

From the current density vector streamline diagram, the variation of streamline density in the Pd catalyst loading region can also be seen. Compared with the region without Pd catalyst, its streamline density increased by a factor of 2.3 (the specific data comparison can be referred to Table 1). This means that the charge transfer efficiency is significantly enhanced under the effect of Pd catalyst, and the electron transfer between the electrode and electrolyte is smoother, which further promotes the electrolytic water reaction. The flow field analysis showed that the flow lines in the Pd catalytic layer showed highly directional transport characteristics, which elucidated that Pd effectively suppressed the disordered migration of ions triggered by the interference of  $\text{Cl}^-$  and  $\text{Ca}^{2+}$  in the electrolysis of seawater through the construction of selective ion channels, providing a key guarantee for the stability of the system.

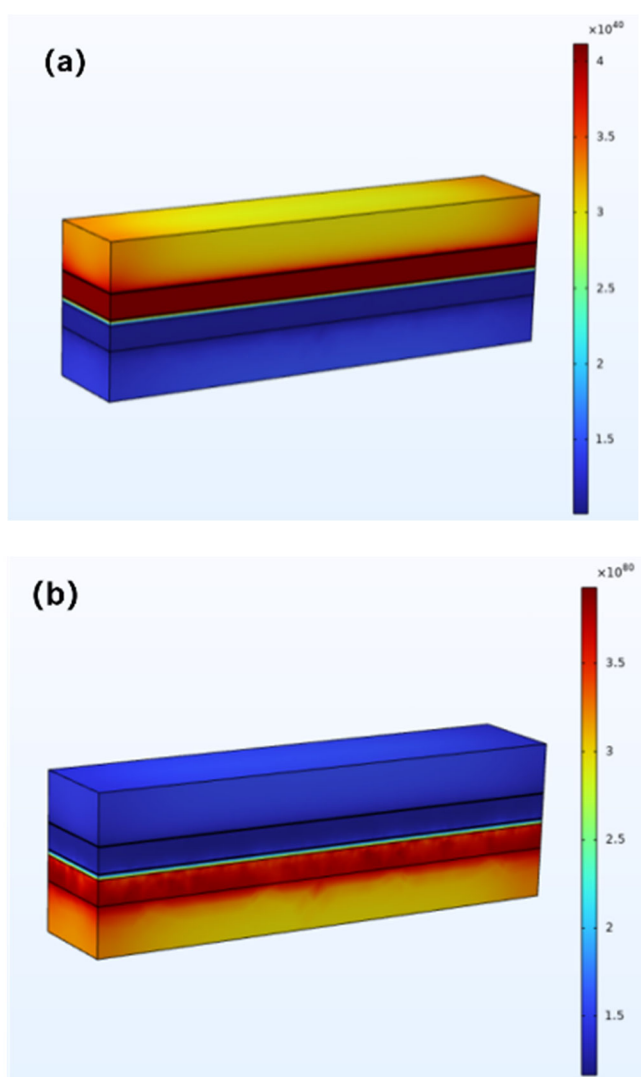


**Figure 6.** (a) Hydrogen molar concentration distribution in steady state,(b) Oxygen molar concentration distribution in steady state

The hydrogen concentration gradient reveals the catalytic activity distribution, and the high concentration zone (in red) corresponds to the Pd active site, as shown in Fig. 6, which shows an obvious quantitative correspondence between the high concentration zone (shown in red) and the active site of the Pd catalyst. In the region with Pd catalyst loading, the hydrogen molar concentration ( $C_{\text{H}_2}$ ) reaches about  $4 \times 10^{40} \text{ mol/m}^3$ , while in the system without Pd catalyst

(shown in blue), the hydrogen molar concentration is only about  $1.5 \times 10^{40}$  mol/m<sup>3</sup>, which indicates that a significant enhancement of hydrogen concentration of 267% is realized in the presence of Pd catalyst (the advantageous comparison of the relevant data can be found in Table 1). This significant increase in concentration intuitively reflects the excellent catalytic ability of the Pd catalyst in promoting hydrogen generation.

The longitudinal gradient distribution feature reveals the advantages of mass transfer kinetics: the continuous incremental trend from bottom to top follows the buoyancy-driven directional transport law, which promotes the efficient enrichment of products at the top of the electrode. The corrosion resistance verified the stable concentration and uniform stratification under seawater environment, and the smooth color transition (no patchy anomalous area) within each horizontal section, indicating that the Pd catalyst suppressed the local reaction stagnation caused by Cl<sup>-</sup> corrosion.

**Table 1.** Performance comparison before and after application of Pd catalysts

Indicator	No Pd catalyst	Pd catalyst	Optimization range
Hydrogen production rate (m <sup>3</sup> /h/kW)	0.45	0.68	+51%
Electrolysis efficiency (%)	62	78	+16%
Energy consumption per unit of hydrogen (kWh/m <sup>3</sup> )	4.8	3.2	-33%
Catalyst life (hours)	3,000	8,500	+183%

Referring to the industry standard "Technical specification of proton exchange membrane electrolysis water hydrogen production system" (GB/T 37562-2019), based on the steady-state/transient simulation results of COMSOL millimeter-scale model, the performance data of Pd catalyst in PEM electrolysis cell can be obtained in comparison with the performance of the system without Pd catalyst, as shown in Table 1, with 51% improvement in the hydrogen production rate, 16% improvement in the electrolysis efficiency, and 33% reduction in the unit hydrogen. The hydrogen production rate is increased by 51%, the electrolysis efficiency is increased by 16 percentage points, the energy consumption per unit of hydrogen is reduced by 33%, the catalyst life is significantly improved, and the energy saving and emission reduction efficacy is remarkable.

#### 4.2. Performance analysis of N-rich ammonia synthesis

From the data in Table 2, it can be seen that the N content of 3DOM g-C<sub>3</sub>N<sub>4</sub> carrier reaches 48.45%, and after the Pd nanoparticles are loaded to form the Pd/3DOM g-C<sub>3</sub>N<sub>4</sub> catalyst, the N content is 48.20%, and the pyridinium N binding energy is shifted to the direction of high binding energy by 0.21 eV, which indicates that the N content of Pd/3DOM g-C<sub>3</sub> catalyst is 48.20% and the pyridinium N binding energy moves to the direction of high binding energy, indicating that the N content of the catalyst is 48.20%. -C<sub>3</sub>N<sub>4</sub> has a strong interaction with Pd, which can effectively activate nitrogen molecules and inhibit hydrogen precipitation reaction by taking advantage of the PdH<sub>x</sub> formation property, and then enhance the efficiency of nitrogen reduction ammonia synthesis.

**Table 2.** XPS data of 3DOM g-C<sub>3</sub>N<sub>4</sub>carrier and Pd/3DOM g-C<sub>3</sub>N<sub>4</sub>catalysts

Sample	N/%	Bindingenergy/eV			GrapheneN/ %	PyrroleN/ %	PyridinetypeN/ %
		GrapheneN	PyrroleN	PyrrolotypeN			
3DOMg-C <sub>3</sub> N <sub>4</sub>	48.45	400.80	399.71	398.26	7.19	17.95	74.85
Pd/3DOMg-C <sub>3</sub> N <sub>4</sub>	48.20	400.85	399.70	398.47	8.13	19.39	72.84

Using COMSOL to simulate the physical field interfaces of laminar flow, surface reaction and dilute material transfer, it is found that the flow lines in the reactor are uniformly distributed without localized dense or dispersed phenomena, which implies that the gas flow is stable, and creates a good condition for the reactants to contact with the catalyst adequately. As can be seen in Fig. 7, the red flow lines are concentrated near the catalyst layer, indicating that the ammonia reaction is most active here. In this area, the active sites of Pd catalyst played a full role and greatly promoted the conversion of N<sub>2</sub> and H<sub>2</sub>.

The simulation results showed that within 5 min after the start of the reaction, the concentrations of the reactants N<sub>2</sub> and H<sub>2</sub> in the vicinity of the catalyst layer decreased rapidly in the presence of the Pd catalyst, while the concentration of NH<sub>3</sub> increased rapidly. By 10 min, the NH<sub>3</sub> concentration reached a steady state, with the NH<sub>3</sub> concentration reaching about 0.06 mol/m<sup>3</sup> in the region near the catalyst layer, compared to the same time without the Pd catalyst, where the N<sub>2</sub> and H<sub>2</sub> concentrations declined slowly and the NH<sub>3</sub> production was minimal, with the NH<sub>3</sub> concentration at 10 min being only about 0.01 mol/m<sup>3</sup>, an increase of 500%.

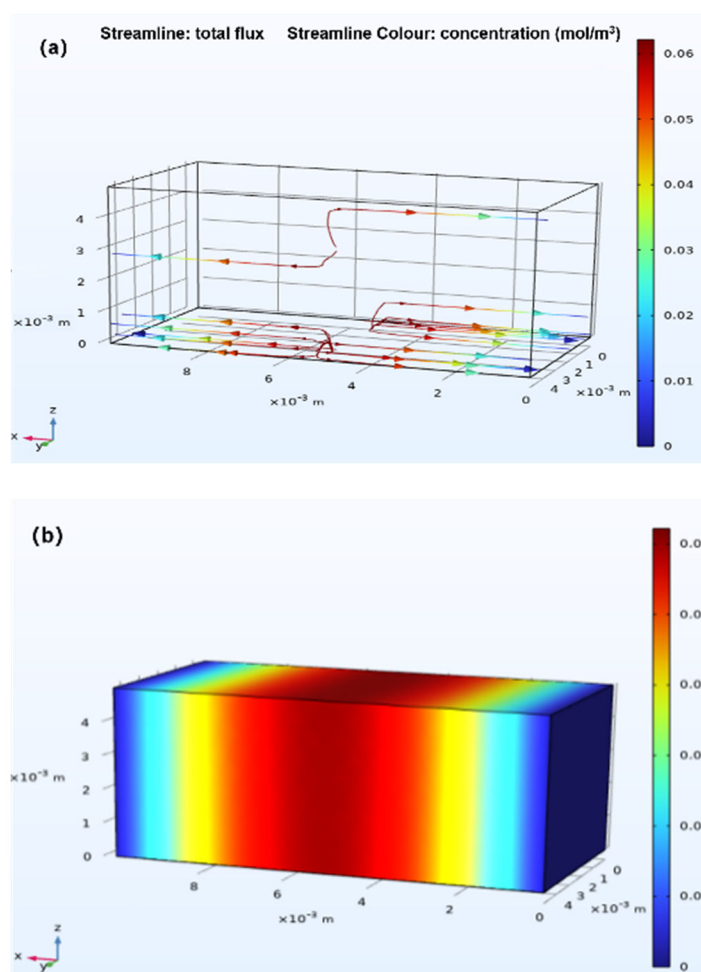


**Figure 7.** (ab) Simulation of Pd/g-C<sub>3</sub>N<sub>4</sub>catalyzed ammonia synthesis reaction

Meanwhile, the 3DOM g-C<sub>3</sub>N<sub>4</sub> carrier provides a good uniform dispersion of Pd nanoparticles to avoid active site aggregation failure. As observed by simulation visualization, in the system with 3DOM g-C<sub>3</sub>N<sub>4</sub> carrier, the Pd nanoparticles were uniformly distributed on the surface of the carrier with more consistent spacing, and each nanoparticle could fully participate in the reaction. In contrast, in the simulated environment without the carrier, the Pd nanoparticles showed obvious agglomeration, and the active sites in the agglomerated regions overlapped and could not function efficiently, leading to a significant reduction in the reaction efficiency.

In addition, the low H<sub>2</sub> concentration indicated that the Pd catalyst effectively inhibited the adsorption and precipitation of H<sub>2</sub> and reduced the side reaction competition. Throughout the simulated reaction, the H<sub>2</sub> concentration in the system with the Pd catalyst remained low and stable at about 0.03 mol/m<sup>3</sup>, whereas it was as high as 0.08 mol/m<sup>3</sup> in the system without the Pd catalyst. Under the low potential condition, the Pd catalyst not only activates the N<sub>2</sub> molecules efficiently, but also achieves high dispersion on the 3DOM g-C<sub>3</sub>N<sub>4</sub> carriers, which successfully forms a localized region of high concentration of NH<sub>3</sub>, and strongly improves the efficiency and quality of ammonia synthesis.

## 5. Conclusions

(1) The hydrogen-ammonia coupling system can stabilize the power supply structure and innovate the energy storage and peak adjustment mode. It can smooth out the fluctuation of offshore wind power due to wind speed fluctuation and operation and maintenance downtime, and convert surplus electricity into hydrogen and ammonia for storage, so as to adjust the peak in the trough of power generation and balance the load of the power grid.

(2) The system can also promote the efficient utilization of wind power and assist in the deep consumption of energy. In wind power-rich areas where grid access is limited, it can reduce wind abandonment, respond to the challenges of stabilization and peak shifting brought about by the increase in the proportion of renewable energy, and provide a feasible path for energy consumption.

## References

- [1] SONG Pengfei, ZHANG Chao, XIAO Li, et al. A review of offshore wind power off-grid consumption and alcohol-ammonia production technologies[J]. Chinese and foreign energy, 2023, 28(11): 16-23.
- [2] Feng Bachuan. Analysis of energy saving and emission reduction in synthetic ammonia industry[J]. Chemical Management, 2019, (22): 35-36.
- [3] Wang Jun. Research on electrocatalysts for ammonia synthesis and decomposition[C]//People's Government of Inner Mongolia Autonomous Region, Chinese Academy of Engineering, China Rare Earth Society, China Rare Earth Industry Association. Abstracts Collection of the 2022 Academic Annual Meeting of the Chinese Society of Rare Earths and the 14th China Baotou-Rare Earth Industry Forum.2022:1.
- [4] Tong Fan, Ji Guangji, Wang Jiajun, et al. Analysis on the coupling system and control mode technology of offshore wind power and PEM electrolyzed water to produce hydrogen[J]. Wind Energy, 2023, (05): 88-97.
- [5] YANG Jingang, LIU Weisie, LI Shunxian, et al. Optimized operation strategy and benefit analysis of wind-hydrogen coupled power generation system[J]. Electric power construction, 2017, 38(1): 106-115.